FET device performance, morphology and X-ray thin film structure of unsubstituted and modified quinquethiophenes

P. Ostoja[a], P. Maccagnani[a], M. Gazzano[b], M. Cavallini[c], J.C. Kengne[c], R. Kshirsagar[a], F. Biscarini[c], M. Melucci[b], M. Zambianchi[b], G. Barbarella[b,*]

[a] *Institute of Microelectronics and Microsystems, Consiglio Nazionale Ricerche, Via Gobetti 101, I-40129 Bologna, Italy*
[b] *Institute for Organic Synthesis and Photoreactivity, Consiglio Nazionale Ricerche, Via Gobetti 101 I-40129 I-Bologna, Italy*
[c] *Institute for Nanostructured Materials Studies, Consiglio Nazionale Ricerche, Via Gobetti 101, I-40129 Bologna, Italy*

Available online 28 September 2004

Abstract

Bottom contact FET devices were realized, using vacuum evaporated thin films of unsubstituted quinquethiophene and two modified derivatives deposited at different substrate temperatures. X-ray diffraction (XRD) and atomic force microscopy (AFM) data on thin films deposited in the same conditions are reported and related to the electrical characteristics of the devices.
© 2004 Elsevier B.V. All rights reserved.

Keywords: FET device; X-ray thin film structure; Atomic Force Microscopy; Quinquethiophenes

1. Introduction

Recently, it has been demonstrated that field effect transistors (FET) fabricated with thiophene oligomers [1,2] can reach charge carrier mobility values in the order of 1×10^{-2} cm^2/V s and I_{on}/I_{off} ratios in the order of $10^6 - 10^7$, which are in the range of the best values obtained so far with organic materials, using pentacene thin films [3] as the active semiconductor layers. Although early measurements on oligothiophenes indicated that charge carrier mobilities should increase on increasing the oligomer size [4–5], more recent experimental evidence indicates very similar mobility values for quater- quinque- and sexithiophenes. [1,6] These results encourage investigations into thin film field-effect transistors based on the shorter thiophene oligomers, such as quinquethiophene (T5, the least investigated oligothiophene; Scheme 1) which are more soluble and, owing to their higher ionization potentials [7] also less susceptible to oxidation.

Recently, we have reported that T5 exhibits a hyerarchical organisation across length scales with highly crystalline thin films characterised by high carrier mobility values [6a]. To

date, no investigation has been carried out on the dependence of the charge carrier mobility of T5 with the morphology of the thin films. Moreover, no systematic studies have been carried out on how structural modifications affect the solid-state organization and the electrical characteristics of odd-number thiophene oligomers. Although, remarkable improvements have recently been achieved on thiophene-based molecular semiconductors, from optimization of device and deposition conditions [5] to material design [8], to the synthesis of *n*-type [9] and ambipolar [10] semiconductors, no clear relationship has as yet been established between molecular structure and electrical performance.

The objective of this paper is to discuss some general trends of variation in the electrical properties of T5 on changing film deposition conditions or introducing structural modifications of the backbone. This work aims to contribute a rationale for the design of new and more performant materials.

2. Experimental

The bottom configuration FET devices used in this study are similar to those described in [6], with interdigitated source and drain gold contacts, channel width and length of 1.1 cm

---
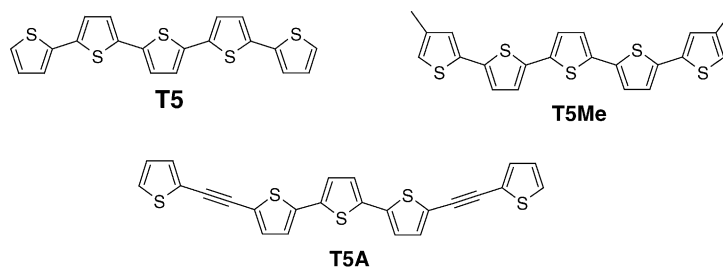
Scheme 1.

and 10 μm, respectively. The SiO$_2$ surface was not functionalised with any primer or chemical treatment. The different oligomers were deposited on the channel region, by vacuum evaporation, at a rate of about 0.1 nm/s. Film thickness was measured during evaporation with a quartz thickness monitor and verified at the end of the process, using a mechanical profiler (Veeco Dektat 6 M). All electrical measurements were performed in ambient atmosphere. All oligomers were purified by silicagel chromatography before use, followed by vacuum sublimation. X-ray diffraction (XRD) measurements were carried out at room temperature, using a Bragg/Brentano diffractometer (Philips PW1050/61-PW1710), equipped with a graphite monochromator in the diffracted beam, with a Cu anode as X-ray source. Atomic force microscopy (AFM) images were obtained with an atomic force microscope (SMENA, NT-MDT, Moscow) operated in air in intermittent contact mode. The cantilevers were silicon cantilevers (NT-NDT NSG10) with high reflective Au coating. The typical curvature radius of the tip was less than 10 nm with a typical resonant frequency of about 255 kHz. Typical relative humidity (RH) during the measurements was controlled with a hygrometer (about 55%).

3. Results

The molecular structure of the oligomers used here is given in Scheme 1. With respect to unsubstituted quinquethiophene (T5), one of the modified derivatives bears two methyl groups (−CH$_3$) grafted at the external β-position (T5Me), while in the other one (T5A) the two terminal thiophene rings are separated from the internal terthiophene core by acetylenic spacers (−C≡C−). The microwave-assisted synthesis, purification methodology and differential scanning calorimetry characteristics of these compounds are reported in references [6a,b]. Of the three compounds, only T5Me displays liquid-crystalline properties [6a,b].

3.1. XRD and AFM

All compounds show a remarkable ability to form highly ordered and crystalline thin films, as shown by the numerous intense high-order reflections in the XRD profiles. The XRD plots of 150 nm thick films of the three samples,

deposited at different substrate temperatures, are shown in Figs. 1–3.

Fig. 1 shows the XRD patterns of two films of T5 deposited at 30 and 90 °C. The same reflections appear in both samples, belonging to two distinct series of peaks with periodicities of 1.92 nm (most intense peaks) and 2.06 nm (peaks indicated by asterisk), respectively, or to multiples of these values. Since the crystal structure previously reported for T5 [11] shows a monoclinic cell with an *a*-axis of 3.9 nm, we can assume the most intense peaks as being due to the *h* 0 0 reflections (*h* even). Although T5 is known for its tendency to form very ordered thin films [6], here the presence of a population of T5 ordered in a slightly different way has to be assumed in order to explain all reflections. The presence of a polymorph
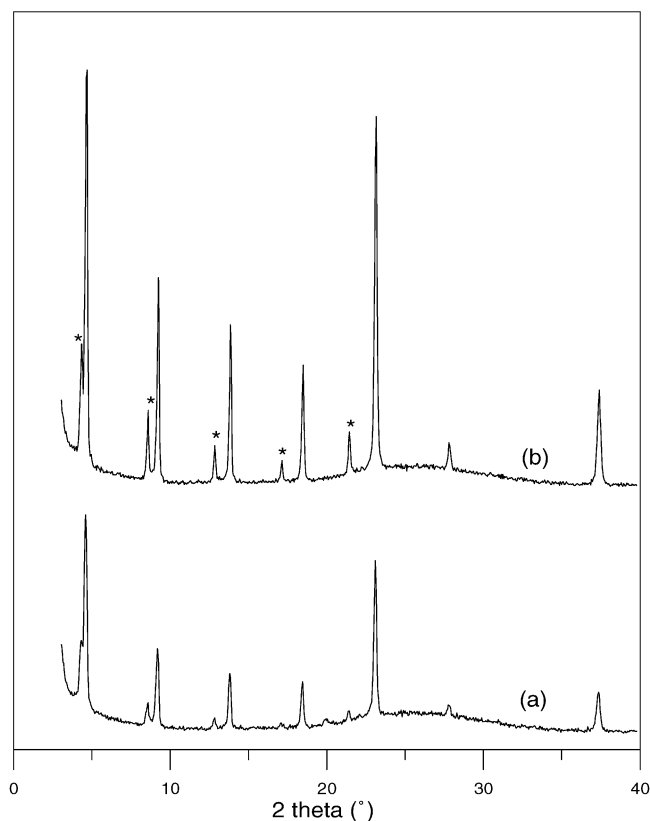

Fig. 1. XRD profile of 150 nm thick films of T5 vacuum evaporated at a substrate deposition temperature of 30 °C (a) and 90 °C (b).
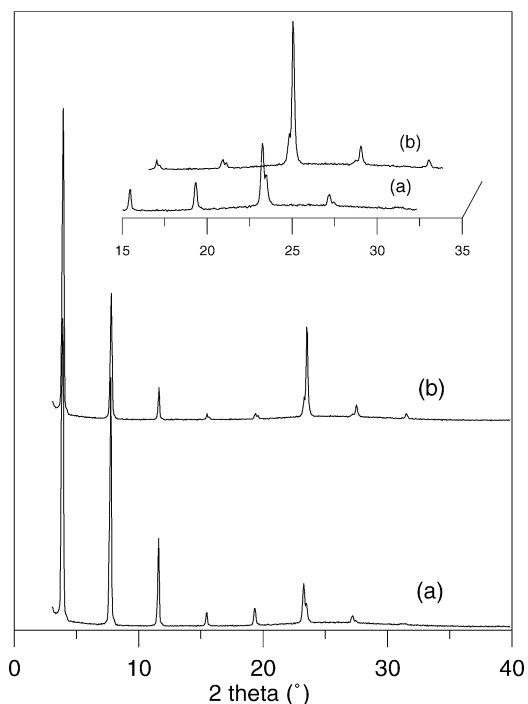
Fig. 2. XRD plots of 150 nm thick films of T5Me for substrate deposition temperatures of 30 (a) and 90 °C (b). The inset is a magnification of the region between 15° and 35° at the two temperatures.

with a different inclination of the molecules with respect to the unit cell axes can be hypothesized. As shown in the figure, the effect of increasing the substrate deposition temperature on T5 is to increase the amount of the minor polymorph in the film. It is worth noting that polymorphs of the shorter and
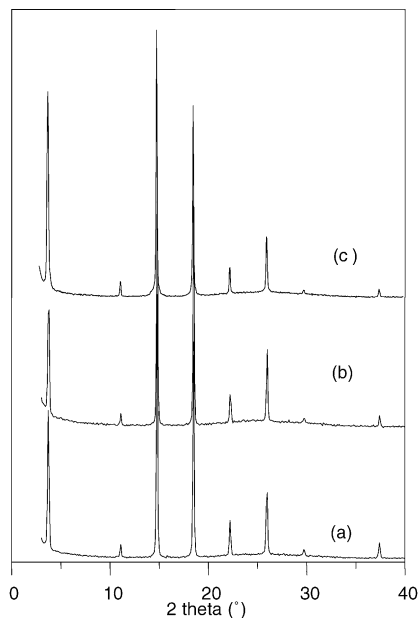

Fig. 3. XRD plots of 150 nm thick films of T5A for substrate deposition temperatures of (a) 30 °C, (b) 90 °C and (c) 140 °C.

the longer homologues of T5, namely, quater- and sexithiophenes, have also been described from single crystal X-ray structures, only differing in the magnitude of the herringbone angle [12,13].

Comparing the peak widths of the films of T5 obtained at the different substrate deposition temperatures, an enlargement of the domain size in the $h\,0\,0$ direction is observed. Application of Scherrer equation [14] allows us to estimate the size of the coherent domains to be 53 and 66 nm for the samples prepared at 30 and 90 °C, respectively.

The XRD patterns of two T5Me samples deposited at different temperatures are shown in Fig. 2. The most intense reflections appear at the same angular positions in both samples and all reveal a periodicity of 2.29 nm (or multiple thereof). They are likely to be of the $h\,0\,0$ kind, although the fact that no single crystal or powder X-ray structures have been reported for this compound makes the assignment somewhat uncertain. Some differences in the diffraction profiles are appreciable for the reflections for 2θ greater than 15°. As reported in the inset of Fig. 2, some reflections are splitted and the relative intensities in each couple is reversed in the samples deposited at the different temperatures. The figure shows that the reflections at the smaller angles are more intense in the substrate deposited at 30 °C.

From the d-spacing values we assume these peaks as higher orders of $h\,0\,0$ type reflections. We used different experimental conditions to test the presence of a splitting also in the reflections for 2θ less than 15°, but with negative results. Therefore, the presence of a second polymorph can be excluded in this case. The more intense reflections at $2\theta > 15°$ for the sample obtained at 90 °C should instead be explained by assuming that a fraction of the sample is oriented in a slightly different way with respect to the substrate. In that case, these reflections should be indexed as $h\,0\,l$ with a large l value. Thus, in the case of T5Me, the effect of increasing the substrate deposition temperature is to change the orientation of some crystalline domains with respect to the substrate. The size of the domains, calculated from the peak width, is not appreciably affected by the deposition temperature, being about 72 nm for both samples.

The XRD patterns of T5A deposited at different substrate temperatures are reported in Fig. 3. Contrary to T5 and T5Me, no changes were observed in the X-ray patterns of the films increasing the substrate deposition temperature up to 140 °C. The figure shows that for $T = 30$, 90 and 140 °C the plots are very similar and consistent with highly crystalline films. The plots are characterized by several reflections, all corresponding to a period of 2.39 nm (or multiple). The reflections are very sharp and it is possible to estimate a size of the crystalline domains of about 100 nm.

The morphology of T5 thin films was imaged by intermittent contact AFM. Fig. 4 shows the AFM images of 15, 80 and 150 nm thick films of T5 deposited at 30, 60 and 90 °C substrate temperatures.

Upon increasing the substrate deposition temperature there is a dramatic change in the morphology of the film.
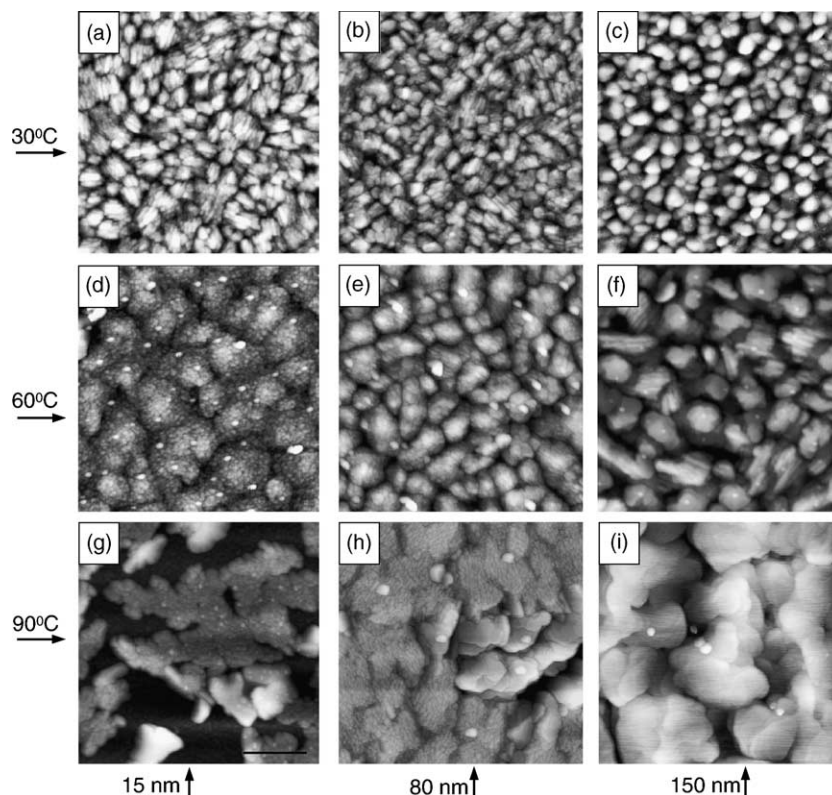
Fig. 4. AFM topographical images of 15, 80 and 150 nm thick films of T5 (z-scale is 0–180 nm, all figures have 3 μm $\times$ 3 μm size) on thermal SiO$_2$. The films were grown at three different substrate deposition temperatures: 30, 60, 90 °C as indicated in the figure.

Fig. 4a–c show the topography of the T5 films grown at 30 °C. The morphology exhibits grains, homogeneously dispersed on the surface. The r.m.s. roughness of the surface is 16 ± 2 nm, almost independent of film thickness and growth temperature. In the thinner films (15 and 80 nm, corresponding to Fig. 4a and b), the clusters appear to be slightly elongated. No ordered layered structure within the grains is observed. However, with the exception of 150 nm thick films, the presence of striped domains inside the clusters is evident. These striped domains have always the same orientation inside a cluster but there is no relation among the stripes orientation of different clusters. The striped domains were already observed in samples prepared by melting-quenching processes of T5 films [6a]. Fig. 5 shows a zoom of the 80 nm thick film grown with a substrate deposition temperature of 30 °C.

The mean diameter of the clusters, measured from the power spectra (Fig. 6a), was 336 ± 20 nm. In order to investigate the spatial correlation of the clusters we compare the power spectral densities (PSD) [15] estimated from the AFM images. All films grown at 30 °C exhibit very similar PSD. Furthermore the PSD shows that the topographic fluctuations are spatially correlated.

Growing the sample at 60 °C (Fig. 4d–f) the shape slightly elongates (this is more evident in the 150 nm thick sample) and the mean diameter, measured from the power spectra

(Fig. 6b), increases in the range 480 ± 20 nm, while the r.m.s. roughness remains almost constant (15 nm). As the thinner films (15 and 80 nm) grown at 30 °C, those grown at 60 °C, do not exhibit an ordered layered structure within the grains. On the contrary, some clusters of the thicker film (150 mm
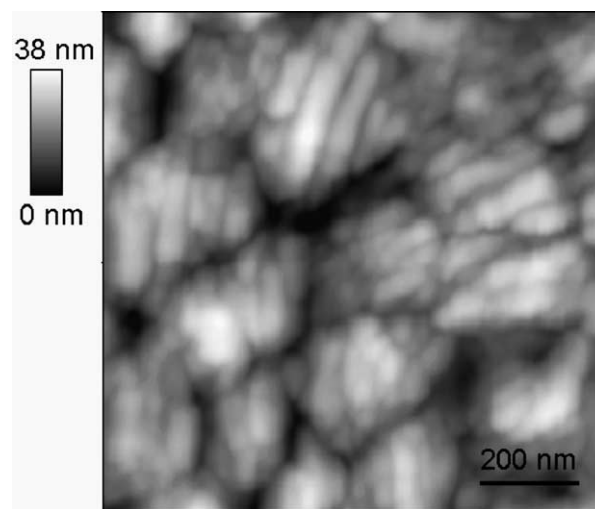

Fig. 5. AFM topographical image of the 80 nm thick film of T5 grown at 30 °C on thermal SiO$_2$. The film exhibits striped domains similar to those already observed in samples prepared by melting-quenching processes [6a].
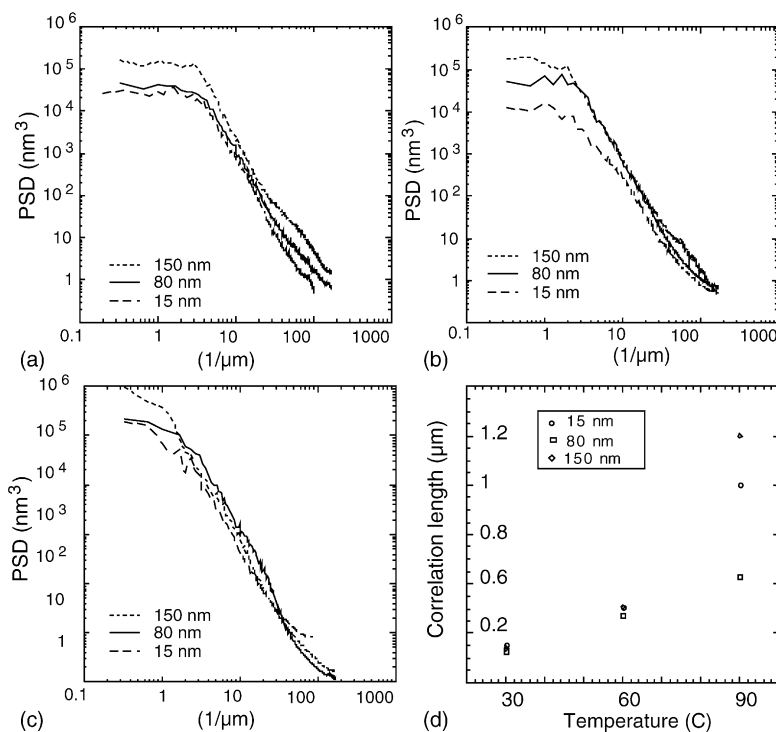
Fig. 6. Power spectral densities measured from the AFM topographic images. (a) Films grown at 30 °C; (b) films grown at 60 °C; (c) films grown at 90 °C. (d) Plot of correlation length vs. deposition temperature.

thick) exhibit small terraces typical of layer-by-layer growth. Furthermore, in this film (Fig. 4f) the striped domains in some clusters are visible. As in the films grown at 30 °C, the PSD plots do not exhibit any significant difference among the films with different thickness (Fig. 6b). At this temperature the PSD plot shows a spatial correlation at high spatial frequency.

In the films grown at 90 °C (Fig. 4g–i), the presence of a terraced structure that is typical of oligothiophene crystals or layered thin films can be observed. The smallest step observed between adjacent terraces was 2.0 ± 0.2 nm, which is consistent with the expected height of a monolayer of T5 molecules (molecular length, 2.2 nm) oriented almost normal with respect to the substrate. The samples exhibit larger islands compared to those of the samples grown at lower temperature, whose size ranges from 0.7 to 1 μm. In the films grown at 90 °C, the striped domains within the grains are not visible. The PSD do not exhibit strong differences among the different thicknesses (Fig. 6c). However, in this case, the spatial correlation is not clear.

Fig. 6d shows the trend of autocorrelation length measured from PSD versus the temperature of film growth. The graph shows a good agreement among the correlation length at 30 and 60 °C, which disappears at high temperature. The plot of correlation length with respect to the deposition temperature (Fig. 6d) shows that the surface exhibits correlation up to 60 °C. At 90 °C, the surface correlation is seen to disappear; further studies are required to investigate the cause of this behaviour. The correlation length is also seen to rise steadily with temperature up to 90 °C.

3.2. Field-effect transistors

Thin film transistors have been realized, using the three different materials at different substrate deposition temperatures (30, 60 and 90 °C). The measurements were performed in air. All compounds showed typical p-type FET behaviour. Examples of the *I–V* characteristics of the devices are reported in Fig. 7 (T5), Fig. 8 (T5Me) and Fig. 9 (T5A).

Table 1 shows the carrier mobilities, I_{on}/I_{off} ratios and threshold voltages for devices obtained with films of T5 of different thicknesses and deposited at different substrate temperatures. The values reported for carrier mobility and threshold voltage are obtained by drawing the square root of the

Table 1

Charge mobility, I_{on}/I_{off} ratio and threshold voltage for T5 as a function of film thickness and substrate deposition temperature

Substrate T (°C)	Thickness (nm)	Carrier mobility ($cm^2/V\,s$)	I_{on}/I_{off}	Threshold voltage (V)
30	15	8.4×10^{-4}	10^4	−0.05
	80	1.7×10^{-2}	10^3	0.8
	150	1.8×10^{-2}	10^3	4
60	15	2.0×10^{-2}	10^2	9
	80	2.7×10^{-2}	10^1	5
	150	1.3×10^{-2}	10^2	6
90	15	9.0×10^{-3}	10^2	3
	80	4.9×10^{-2}	10^1	20
	150	7.8×10^{-2}	10^2	23
140	150	2.2×10^{-2}	10^1	5

Fig. 7. *Left*: Plot of the drain current I_D vs. drain voltage V_{DS} at different gate voltages (V_{GS}) obtained for a 150 nm thick film of T5A deposited at a substrate T of 30 °C. *Right*: Semilogarithmic plot of I_D vs. V_{GS} at $V_{DS} = -10$ V.
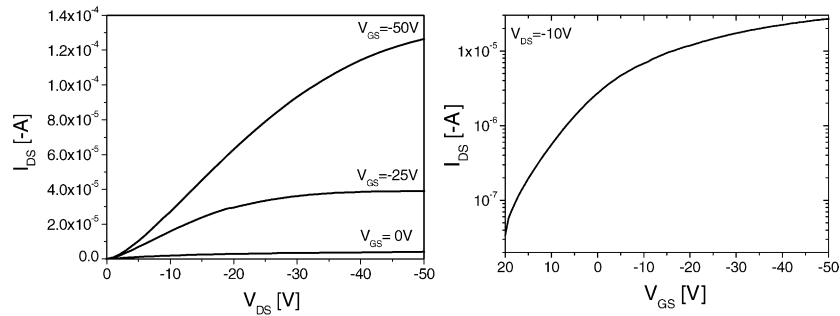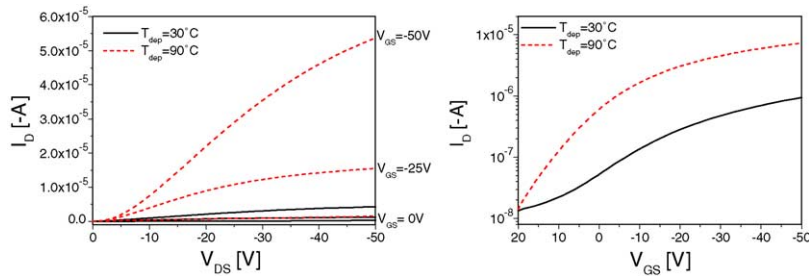

Fig. 8. *Left*: Plot of the drain current I_D vs. drain voltage V_{DS} at different gate voltages (V_{GS}) obtained for a 80 nm thick film of T5 deposited at a substrate T of 30 °C. *Right*: Semilogarithmic plot of I_D vs. V_{GS} voltage at $V_{DS} = -10$ V.

saturation current (taken at $V_{DS} = V_{GS}$) as a function of the gate voltage. Indeed, in the saturation regime, the expression of the drain current can be simplified, assuming that dopant and carrier concentration are equal, as in (1):

$$I_{D,sat} = \frac{W \mu C_i (V_{GS} - V_T)^2}{2L} \tag{1}$$

In Eq. (1), C_i is the insulator capacitance per unit area (5.16 nF/cm^2), W and L the channel width and length, respectively, and V_T is the threshold voltage. From (1) a value for the carrier mobility is obtained assuming a constant mobility [16].

As shown in the table, the carrier mobility of T5 is always around 10^{-2} cm^2/V s. The only film with a lower mobility value is the 15 nm thick one deposited at 30 °C.

For the thicker T5 films (80 and 150 nm) we observe a slight and progressive increase in carrier mobility with substrate deposition temperature up to 7.8×10^{-2} cm^2/V s, which is the highest value reported so far for this compound. The value of threshold voltage is near 0 V for the films deposited at room temperature (4 V for the thicker film) and increases with the deposition temperature, reaching 20 V at 90 °C. Similarly, the I_{on}/I_{off} ratio decreases at higher deposition temperatures, due to the higher conduction of the FET device.

Carrier mobilities, I_{on}/I_{off} ratios and threshold voltages for devices obtained with 150 nm thick films of T5Me and T5A deposited at different temperatures, are given in Table 2.

Both compounds display much lower charge mobilities than T5, with a trend towards higher mobilities on increasing

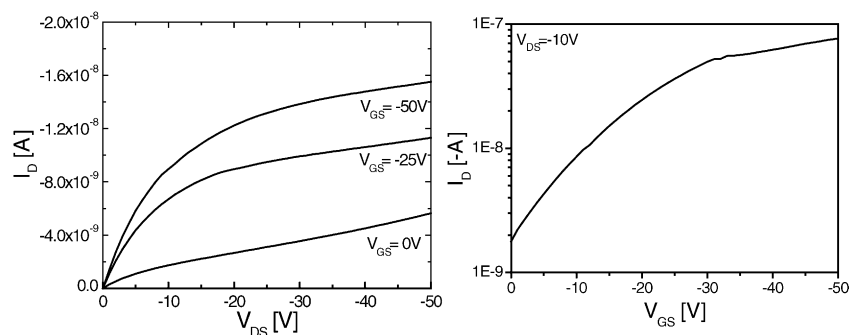Fig. 9. *Left*: Plot of the drain current I_D vs. drain voltage V_{DS} at different gate voltages (V_{GS}) obtained for a 150 nm thick film of T5Me deposited at a substrate T of 30 °C (continuous line) and at 90 °C (dotted line). *Right*: Semilogarithmic plot of I_D vs. V_{GS} at $V_{DS} = -10$ V.

Table 2
Charge mobility, I_{on}/I_{off} ratio and threshold voltage of T5Me and T5A as a function of substrate temperature

	Substrate $T\,(°C)$	Carrier mobility $(cm^2/V\,s)$	I_{on}/I_{off}	Threshold voltage (V)
T5Me	30	7.5×10^{-4}	10^2	−5
	60	1.6×10^{-3}	10^2	−5
	90	9.2×10^{-3}	10^3	−5
T5A	30	4×10^{-6}	10^1	
	60	9×10^{-6}	10^1	
	90	2×10^{-5}	10^2	
	140	8×10^{-4}	10^1	

Film thickness is 150 nm.

the substrate deposition temperature, more accentuated than in T5.

We can observe that the introduction of structural modification in the aromatic backbone affects the carrier mobility of the material. In particular, introducing two methyl groups at the β-terminal positions, the carrier mobility is two orders of magnitude smaller than that of T5, while introducing acetilenic spacers lowers the carrier mobility of almost four orders of magnitude. Moreover, Table 2 shows that the threshold voltage of T5Me does not change with temperature.

4. Discussion

It is well known that the vacuum evaporated thin films of thiophene oligomers tend to orient with the long axis perpendicular to the substrate, with a tilt angle with respect to the normal, which depends on the molecular structure and deposition conditions and that charge transport occurs preferentially in plane [17,1–2,6].

XRD and AFM measurements performed on T5 offer a key to interpreting the trend of variation of the electrical characteristics of the FET devices on increasing the substrate deposition temperature of the active layers.

First of all, the AFM image reported in Fig. 4a indicates that the low carrier mobility (8.4×10^{-4} cm^2/V s) of the 15 nm thick film of T5 grown at a substrate deposition temperature of 30 °C is due to an incomplete surface coverage. For all the other films the carrier mobility varies in the range $\sim 1 \times 10^{-2}$ to $\sim 8 \times 10^{-2}$ cm^2/V s, the highest value being that of the 150 nm thick film grown at 90 °C. For this film, the AFM image shows the presence of a terraced structure typical of layered thin films, with the smallest step between adjacent terraces being consistent with the height of a monolayer of T5 molecules almost upright to the substrate. The fact that the film displays a mobility value of $\sim 8 \times 10^{-2}$ cm^2/V s, the highest reported so far for T5, suggests that also the few first layers of the film are organized in the same way. Indeed, it has been demonstrated that in sexithiophene the charge mobility is controlled by the first two monolayers. [15b] However, since in bottom contact FETs the carrier injection is limited to thin lines along the edges of the contacts, it cannot be ex-

cluded that a further contribution to the charge mobility of the film also comes from the presence of larger crystalline domains (as indicated both by XRD and AFM), which allow a more efficient carrier injection and smaller contact resistance.

We relate the increase of "off" currents observed in T5 FET devices (Table 1), on increasing the substrate deposition temperature, to the increase in the amount of a second crystalline form of T5, revealed by XRD of thin films deposited at the same temperatures. As shown in Table 1, the presence of a second polymorph has only a small effect on the carrier mobility of T5. However, the growth of the amount of the minority polymorph of T5 on increasing the substrate deposition temperature reduces the degree of order in the film and hence increases the density of structural defects acting as traps in the device. The presence of the traps comes out from the analysis of the threshold voltage values (V_T) of the devices. Indeed, as the oligomer is undoped, the shift of V_T from 0 V towards more positive values can be ascribed to charged defects at the oligomer–SiO$_2$ interface. Table 1 shows that for the film deposited at room temperature, V_T is closed to 0 V (4 V for the thicker film) indicating that both the oxide and the oligomer are relatively free of charge defects, while V_T values increase up to 20 V for deposition at 90 °C. Moreover, the shift of V_T towards large positive values is strictly related to the lowering of the I_{on}/I_{off} ratio, which is due to the higher conduction of the device. It is worth noting that it has recently been demonstrated that carrier transport in thiophene oligomers is traps dominated [2].

Despite the fact that the electronic structure of the frontier orbitals of T5Me and T5A are very similar to those of T5 [6] and despite the highly crystalline nature and larger domains size of their thin films, as determined by XRD, their carrier mobilities are lower than that of T5 by several orders of magnitude (Table 2). The increase of the deposition temperature causes much larger increases in the carrier mobilities of these compounds.

Also in the case of T5Me, XRD data offer a clue to understand the electrical behaviour of the FET device. XRD data show indeed that the increase in deposition temperature causes the reorientation of some crystalline domains. The rearrangement of the material with the deposition temperature is accompanied by a marked increase in the carrier mobility. On the contrary, the threshold voltage is not affected by the temperature, indicating that in the film the temperature change does not cause the increase of charge traps. On the basis of these data, one can infer that the increase in the deposition temperature leads to a more homogeneous alignment and a better stacking of the T5Me molecules with respect to the substrate, thus favouring the carrier mobility.

Probably, this is also the reason why we observe the increase in the carrier mobility with the substrate temperature in T5A. However, in this case, no indications come from XRD plots, which remain the same even at 140 °C. Also, the domain size, around 100 nm as measured by XRD, much larger than that of T5 and T5Me, does not show any variation with

temperature. Since, the low carrier mobilities measured for this compound cannot be ascribed to the lack of film crystallinity or to the smaller size of crystalline domains, other factors, such as a poor overlap of the electronic wave functions within the transport layer, related to a looser packing caused by the different molecular shape (Scheme 1), have to be invoked. An indication in this direction comes from the photoluminescence quantum yield of T5A, which is roughly one order of magnitude greater than that of T5. In thiophene oligomers the photoluminescence in the solid state is generally very low owing to the close molecular packing. Work is currently in progress to elucidate this point.

In conclusion, our data show that in T5 the presence of a second polymorph leads to a remarkable decrease of the I_{on}/I_{off} values, whereas it does not affect the carrier mobility values. Substitution of methyl groups at the terminal positions, as in T5Me, or the introduction of acetilenic spacers, as in T5A, prevents the formation of polymorphs but leads to a remarkable decrease in carrier mobility. In the case of T5Me, XRD data indicate that the increase in the substrate deposition temperature affects the orientation of the crystalline domains with respect to the substrate, in a direction that is favourable to the increase of carrier mobility. These data suggest that the good results achieved with oligothiophenes terminated by long alkyl chains [1] are related both to the absence of polymorphs and to the homogeneous orientation of the crystalline domains with respect to the substrate.

We believe that systematic electrical characterization of libraries of purposely synthesized molecules, paralleled by thin film XRD and AFM measurements, will allow the different factors contributing to charge transport, from the energy of HOMO and LUMO frontier orbitals to crystalline domains size and orientation to intermolecular overlap of the electronic wave functions - to be disentangled. In this way, it will be possible to establish the molecular structure/electrical properties relationships that will allow the rationale design of better performing materials.

Acknowledgments

References

[1] M. Halik, H. Klauk, U. Zshieschang, G. Schmid, S. Ponomarenko, S. Kyrchmeyer, Adv. Mater. 15 (2003) 917–922.

[2] S. Mohapatra, B.T. Holmes, C.R. Newman, C.F. Prendergast, C.D. Frisbie, M.D. Ward, Adv. Funct. Mater. 14 (2004) 605–609.

[3] (a) T.W. Kelley, D.V. Muyres, P.F. Baude, T.P. Smith, T.D. Jones, Mater. Res. Soc. Symp. Proc. 771 (2003) L6.5.1–L6.5.11;
(b) H. Meng, M. Bendikov, G. Mitchell, R. Helgeson, F. Wudl, Z. Bao, T. Siegrist, C. Kloc, C.H. Chen, Adv. Mater. 15 (2003) 1090–1093;
(c) S.E. Fritz, S.M. Martin, C.D. Frisbie, M.D. Ward, M.F. Toney, J. Am. Chem. Soc. 126 (2004) 4084–4085.

[4] (a) R. Hajlaoui, G. Horowitz, F. Garnier, A. ArceBrouchet, L. Laigre, A. ElKassmi, F. Demanze, F. Kouki, Adv. Mater. 9 (1997) 389–393;
(b) R. Hajlaoui, D. Fichou, G. Horowitz, B. Nessakh, M. Constant, F. Garnier, Adv. Mater. 9 (1997) 557–561.

[5] C.D. Dimitrakopoulos, P.R.L. Malenfant, Adv. Mater. 14 (2002) 99–117.

[6] (a) M. Melucci, M. Gazzano, G. Barbarella, M. Cavallini, F. Biscarini, P. Maccagnani, P. Ostoja, J. Am. Chem. Soc. 125 (2003) 10266–10274;
(b) M. Melucci, G. Barbarella, M. Zambianchi, P. Di Pietro, A. Bongini, J. Org. Chem. 2004 (ASAP article).

[7] (a) D. Jones, M. Guerra, L. Favaretto, A. Modelli, M. Fabrizio, G. Distefano, J. Phys. Chem. 94 (1990) 5761–5766;
(b) K. Meerholiz, J. Heinze, Electrochim. Acta 41 (1996) 1839–1843.

[8] A.R. Murphy, J.M.J. Fréchet, P. Chang, J. Lee, V. Subramanian, J. Am. Chem. Soc. 126 (2004) 1596–1597.

[9] R.J. Chesterfield, C.R. Newman, T.M. Pappenfus, P.C. Ewbank, M.H. Haukaas, K.R. Mann, L.L. Miller, C.D. Frisbie, Adv. Mater. 15 (2003) 1278–1282.

[10] A. Facchetti, M.H. Yoon, C.L. Stern, H.E. Katz, T.J. Marks, Angew Chem. Int. Ed. 42 (2003) 3900–3903.

[11] W. Porzio, S. Destri, M. Mascherpa, S. Brückner, Acta Polym. 44 (1993) 266–272.

[12] (a) L. Antolini, G. Horowitz, F. Kouki, F. Garnier, Adv. Mater. 10 (1998) 382–385;
(b) T. Siegrist, C. Kloc, R.A. Laudise, H.E. Katz, R.C. Haddon, Adv. Mater. 10 (1998) 379–382.

[13] (a) G. Horowitz, B. Bachet, A. Yassar, P. Lang, F. Demanze, J.L. Fave, F. Garnier, Chem. Mater. 7 (1995) 1337–1341;
(b) T. Siegrist, R.M. Fleming, R.C. Haddon, R.A. Laudise, A.J. Lovinger, H.E. Katz, P. Bridenbaugh, D.D. Davis, J. Mater. Res. 10 (1995) 2170–2173.

[14] H.P. Klug, L.E. Alexander, XRD Procedures for Polycrystalline and Amorphous Materials, Wiley-Interscience, New York, 1974;
The line broadening was used to evaluate the length of the coherent domains (τ_{hkl}). τ_{hkl} values were calculated from the widths at half maximum intensity ($\beta_{1/2}$) using the Scherrer equation: $\tau_{hkl} = k\lambda/\beta_{1/2}\cos\theta$, where λ is the wavelength, θ the diffraction angle and k a constant depending on crystal habit (chosen as 1.0). The instrumental broadening was taken into account, the strain of crystalline lattice was neglected.

[15] (a) F. Biscarini, P. Samori, O. Greco, R. Zamboni, Phys. Rev. Lett. 78 (1997) 2389–2392;
(b) F. Dinelli, M. Murgia, P. Levy, M. Cavallini, F. Biscarini, D.M. de Leeuw, Phys. Rev. Lett. 92 (2004) 1168021–1168024.

[16] G. Horowitz, Physics of organic field-effect transistors, in: G. Hadziioannou, P.F. van Hutten (Eds.), Semiconducting Polymers, Wiley, 2000, p. 463.

[17] F. Garnier, A. Yassar, R. Hajlaoui, G. Horowitz, F. Deloffre, B. Servet, S. Ries, P. Alnot, J. Am. Chem. Soc. 115 (1993) 8716–8721.